Master degree on nanostructured materials for nanotechnology applications

FINAL MASTER PROJECT

Use of organic compounds in molecular electronics

JAVIER CORTÉS CAMEROS

ZARAGOZA, SEPTIEMBRE DE 2013

PILAR CEA MINGUEZA, profesora titular del Departamento de Química Física de la Universidad de Zaragoza y SANTIAGO MARTÍN SOLÁNS, profesor ayudante doctor del Departamento de Química Física de dicha Universidad

CERTIFICAN:

Que el trabajo presentado en esta memoria por Javier Cortés Cameros como Proyecto Final del Máster Universitario en Materiales Nanoestructurados para Aplicaciones Nanotecnológicas y que lleva como título *"Use of organic compounds in molecular electronics"*, ha sido realizado en el Departamento de Química Física de la Facultad de Ciencias de la Universidad de Zaragoza, bajo su dirección, autorizando la presentación del mismo para su calificación por el Tribunal correspondiente.

Y para que así conste, se expide el presente certificado en Zaragoza, a 9 de septiembre de 2013.

Fdo: Pilar Cea Mingueza

Fdo: Santiago Martín Soláns

Agradecimientos

Parece que fue ayer cuando empecé en esta Universidad la carrera, pero no, ya han pasado seis años, seis años maravillosos que terminan con este trabajo fin de máster (TFM). A lo largo de este tiempo en el que he realizado mi licenciatura en Química y este máster, he vivido momentos fantásticos, tanto personal como científicamente, lo cual me ha ayudado también para mejorar e intentar superarme cada día en ambos campos. Así, dado que este TFM supone para mí el final de una etapa de mi vida, estas líneas son de agradecimiento por estos seis años vividos en esta Facultad de Ciencias de la Universidad de Zaragoza.

En primer lugar me gustaría agradecer al grupo PLATÓN del Departamento de Química Física la oportunidad que me ha brindado al poder realizar el TFM con ellos. Agradezco asimismo al Laboratorio de Microscopías Avanzadas (LMA) y al Instituto de Nanociencia de Aragón (INA) la posibilidad de usar sus infraestructuras. Igualmente cabe agradecer aquí la financiación del proyecto del Ministerio de Economía y Competitividad CTQ2009-13024 y del nuevo CTQ2012-33198. Por último, agradecer también a la cátedra SAMCA la concesión una beca que cubrió parte de los gastos de matrícula del máster. Gracias a este año de duro trabajo salgo de aquí con una base de conocimientos científicos más amplia y profunda.

Un lugar muy importante y preferente es para mi codirectora de TFM, la Dra. Pilar Cea Mingueza. Muchísimas gracias por permitirme realizar este trabajo en vuestro grupo, y por todo lo que he aprendido, pero no sólo en el ámbito científico, sino el personal, para mí mucho más importante. Por todos tus consejos, ayudas y opiniones, no sólo este curso, sino durante todos estos años. Me llevo muchas cosas aprendidas, pero sobre todo, me llevo para siempre una gran amiga. GRACIAS.

Otro lugar especial e importante es para mi codirector de TFM, el Dr. Santiago Martín Soláns. Muchísimas gracias también por permitirme desarrollar este trabajo con vosotros. Siempre atento a cualquier cosa que necesitara, ayudándome en todo lo que hiciera falta, dándome buenos consejos, facilitando mi tarea y ayudándome a mejorar día a día. GRACIAS por todo, me llevo de aquí otro gran amigo.

A mis compañeros de laboratorio y profesores del grupo PLATÓN con los que he compartido tantas y tantas horas a lo largo de este trabajo, gracias por hacerme disfrutar de este año, con un ambiente de trabajo que es inigualable.

Por supuesto, no podía olvidarme en este momento de mi familia. Agradecer a mis padres, Vicente y Caty, TODO. No sabría expresar con palabras lo que para mí significan mis padres, lo que me han enseñado, la educación que me han dado, los valores que me han proporcionado, la cantidad de cosas que han realizado por mi hermana y por mí, muchas veces incluso privándose de disfrutar ellos. Por todo ello, por estar siempre en todos los momentos de mi vida, en los buenos y en los malos, por apoyarme siempre, por todo lo que nos queda por vivir, que espero que sea todavía mucho más que lo andado; en definitiva, por ser el sustento, soporte y alimento de mi vida, MUCHÍSIMAS GRACIAS.

Asimismo, me quiero acordar de mi hermana, Arantxa. Por todos estos años que hemos vivido juntos, en especial los últimos seis aquí en Zaragoza tu y yo solos, por los buenos ratos que hemos pasado, desde niños hasta hoy, y los que nos quedan, por ayudarme en todo lo que he necesitado, y por tantas y tantas cosas, GRACIAS.

A David y Trasto, agradeceros todo lo que habéis hecho por mí, en especial, por intentar sacarme una sonrisa cuando me enfado, pero sobre todo, por hacer feliz a mi hermana.

A mis amigos de Alfaro, muchísimas gracias por todos estos años, desde el colegio hasta hoy en día. Aunque muchas veces no les puedo dedicar el tiempo que me gustaría, ellos me comprenden, saben que son una parte muy importante de mi vida y siempre que los necesito están ahí.

A mis amigos de Zaragoza, mostraros mi gratitud por estos seis años que he vivido con vosotros. Espero que nunca se pierda la relación que tenemos y que con el tiempo sigamos viéndonos y recordando estos preciosos años de nuestras vidas.

Hay tantas personas a las que tengo que darles las gracias que no acabaría nunca. Por ello, para todos aquellos que no he nombrado, pero que habéis formado parte de esta experiencia inolvidable de mi vida, gracias.

Index

Abstract 1

Chapter 1: Objectives 3

1.1. General objectives 3

1.2. Objectives of the final master project "Use of organic compounds in molecular electronics" 4

Chapter 2: Introduction and revision of the state of the art 5

2.1. Introduction 5

2.2. Revision of the state of the art 5

Chapter 3: Instrumentation and materials 13

3.1. Instrumentation 13

3.1.1. Fabrication of Langmuir and Langmuir-Blodgett (LB) monolayers 13

3.1.2. Characterization of the Langmuir-Blodgett (LB) films 14

3.1.3. Electrical properties of the Langmuir-Blodgett (LB) films 15

3.2. Materials 16

Chapter 4: Electrical properties of FOSGAC and G-PEA 21

4.1. Langmuir and Langmuir-Blodgett (LB) monolayers and the fabrication of the top-contact electrode 21

4.2. Electrical measurements 24

Chapter 5: Graphene as top-contact electrode in molecular electronics 31

Chapter 6: Conclusions 41

Chapter 7: References 43

Abstract

Nowadays, the current electronic industry based on silicon is near to its limit. Thus, many different alternatives are being investigated to continue decreasing the size of the chips and improving, at the same time, the efficiency, efficacy and power. One of these alternatives is molecular electronics, whose final goal is the use of individual molecules or a few of them to fabricate electronic devices. In contrast with silicon electronic industry, molecular electronics is based on bottom-up techniques and its origin is in the last seventies although before being a reality, many challenges have still to be overcome as it has been indicated by ITRS (*International Roadmap for Semiconductors*). Some of these challenges, which are directly related with this final master project, are: (i) fabrication of robust contacts between the metals and the organic molecules; (ii) fabrication of the top-contact electrode on monomolecular layers without damaging the organic molecule and penetrating the film; and (iii) have a deep knowledge of the charge transport mechanisms through the organic compounds.

Taking into account the foregoing challenges, in this project four different compounds have been used to contribute to this field, in particular to the fabrication of the top-contact electrode. First, the top-contact electrode was fabricated by the rupture of an organometallic compound immobilized onto a gold substrate, induced by thermal annealing, and the electrical properties of the devices were determined with a conductive-AFM (chapter 4). Since short-circuits have not been observed using this method, this strategy is an alternative technique for solving the top-contact electrode problem without damaging the organic molecule, penetrating the film or altering/contaminating the interfaces. Second, a top-contact electrode was prepared by chemical reduction of a graphene oxide layer transferred onto a monolayer of an organic compound by means of the Langmuir-Blodgett (LB) technique (chapter 5). Thus, metal | SOPEA LB film | reduced graphene oxide (RGO) structures have been fabricated as it has been demonstrated by UV-Vis spectroscopy, QCM and AFM.

Chapter 1: Objectives

1.1. General objectives

The objectives of a final master project of the Master´s Degree in Nanostructured Materials for Nanotechnology Applications from the University of Zaragoza are the acquisition and consolidation by the student of basic skills in nanomaterials and nanotechnology.

Among these basic skills, the student should be able to: sorting, critically analyze, interpreting, and synthesizing information; obtaining information from different types of sources and assess their reliability; applying knowledge and solving problems related to the study area; integrating knowledge and addressing the complexity of making judgments based on information that, being incomplete or limited, including reflexions on social and ethical responsibilities linked to the application of their knowledge and judgments; develop, analyzing, evaluating and comparing new or alternative solutions to various problems; being able to develop a project, the steps involved in literature search, planning experiments, obtaining results, interpretation, and dissemination of the results; managing properly the resources and time available; communicating own conclusions clear and unambiguous to specialist and non-specialist public; giving information orally, written or graphic presentation using appropriate tools; communicating fluently in English; using the vocabulary and specific terminology in the context of nanoscience and nanotechnology; knowing the degree of importance of researches and industrial applications of nanoscience and/or nanotechnology and its social, economic, and legal implications; interrelating the chemical structure, the architecture or the arrangement of nanostructured material with its chemical, physical, optical and mechanical properties; knowing the fabrication methods of nanostructured materials, bottom-up and top-down approaches; knowing the characterization methods of nanostructured materials, the type of information provided by each one and how it can be used in a complementary way to obtain the required information; designing of new materials and biomaterials with interest in nanoscience and / or nanotechnology; and applying theoretical knowledge for making nanodevices.

1.2. Objectives of the final master project *"Use of organic compounds in molecular electronics"*

This project has two main objectives:

- Determination of the electrical properties of metal | organic monolayer | metal junctions which were fabricated by thermal induced decomposition of organometallic compounds incorporated in Langmuir-Blodgett (LB) films.

- To develop a new strategy to fabricate the top-contact electrode without damaging or penetrating the organic monolayer in metal | organic monolayer structures by deposition of a graphene film in ambient conditions.

Chapter 2: Introduction and revision of the state of the art

2.1. Introduction

In the next section, a brief review of the state of the art on molecular electronics is presented. In chapter 3, the instruments and materials used in this work are described. In chapter 4, the electrical properties of the fabricated metal | organic molecule | metal junctions are determined while in chapter 5, graphene is presented as a new possible alternative for making the top-contact electrode. Finally, chapter 6 describes the main conclusions of this work.

2.2. Revision of the state of the art

In the 20th century and in the first decade of the present century, the electronic industry has suffered an important development as consequence of a continue miniaturization of the elements and components used for making electronic devices. This process of miniaturization has been made using top-down techniques, which progressively reduce the size of devices using sophisticated photolithographic techniques. Nevertheless, the limit of the actual electronic industry based on silicon is achieving its limit[1-3] by reasons both technological and economical.[4-6] From the economic point of view, each generation of chips requires the construction of a new manufacturing system, which is very expensive, and the companies have few months to make profitable the inversion. From the technological point of view, metal oxide layers with a thickness less to three atoms lose their insulating properties and short-circuits are easily produced. In addition, silicon does not preserve its band structure, so it is really difficult to continue the miniaturization process by top-down techniques.

For all these reasons, several alternatives to the current electronic industry are being developed. One of these possible alternatives is molecular electronics, a bottom-up based technology that uses functionalized individual molecules that work as wires, switches, rectifiers, memories, etc.[7-9] To achieve this objective it will be necessary to measure, monitor and understand the electronic transport through molecules situated between electrodes. Specifically, molecular electronics consists on devices involving a single molecule, or a monolayer, oriented between two electrodes (which may be conductors or semiconductors).[10,11] Thus, the use of organic molecules in electronic components could provide, at least, the following advantages:[4,12,13] (i) the small size of the molecules could lead to devices with higher packing densities, and therefore, lower costs and higher efficiency; (ii) molecular recognition and assembly get to fabricate nanoscale structures through specific intermolecular interactions between the molecules, obtaining low manufacturing costs; (iii) this molecular recognition can be used to modify the electronic behavior; (iv) the speed of response would increase, so the time required for an operation would be reduced; (v) special properties of the molecules such as different geometric structures or isomers, getting new electronic behaviors that cannot be implemented in conventional solid state devices; and (vi) the transport properties and specific properties of the molecules can be modified extensively with an appropriate design of the chemical composition and molecular geometry. However, the molecules have also some disadvantages such as the instability at high temperatures. Besides, the fabrication of good molecular junctions requires a precise control of the matter at unprecedented levels which can be difficult, slow and expensive. Nevertheless, these difficulties are not strong enough to discourage scientists to continue using molecular materials in electronic applications.

In recent years, many different investigations have demonstrated that organic molecules lead and switch electric current and also act as memory devices which provide a solid basis to continue the development of molecular electronics. However, we are still very far to assembly a chip using these materials, although the possibilities are amazing.[14-16] Molecular electronics is still on its infancy and many challenges have to be overcome before it becomes as it has been indicated by the ITRS (*International Technology Roadmap for Semiconductors*). Among the challenges set by the ITRS,[17] two are directly related with the work carried out in this work: (i) fabrication of stable

and suitable metal | organic molecule | metal junctions using new strategies to fabricate the top-contact electrode on monomolecular films without damaging the organic compound or penetrating the film, and (ii) measuring the electrical properties of these metal | organic films | metal devices without having short-circuits which verify that these new strategies are an alternative system for solving the top-contact electrode problem without damaging the organic molecule, penetrating the film or altering/contaminating the interfaces.

Taking into account the two objectives of this work, in the next paragraphs a revision of the techniques used to carry out the electrical characterization of metal | molecule | metal devices together with a revision of the state of the art in the fabrication of the top-contact electrode are presented.

1- *Determination of the electrical properties:*

In recent years, a wide variety of techniques for measuring the electrical properties in metal | organic layer | metal sandwiches have been developed. In the next lines, some of the most used and important methods for analyzing these structures are explained briefly.

Nowadays, the most important instruments for measuring the electrical properties of single molecules or monolayers are the scanning probes microscopies (SPM): a scanning tunneling microscopy (STM) and/or a conducting atomic force microscopy (c-AFM). In both cases, the tip acts as the top-contact electrode closing the circuit in the metal | organic molecule | metal junctions. The main advantage of these instruments is that a large amount of electrical measurements can be collected in a short time. A STM can work in current mode, constant height, or as a combination of both, allowing recording the tunnel current and topography of a sample at atomic scale simultaneously. Thus, this is a visual and simple method for studying the molecular conductance. In the case of a c-AFM, the tip, coated with a metallic layer, is placed in direct mechanical contact with the molecules on a thorough survey of the position of the AFM tip, to avoid an excessive pressure on the molecules that can change their conformation and thus the transport properties; this avoids the extra space or air gap that can present the use of a STM. The c-AFM technique provides a simple and

convenient way to fabricate molecular junctions and study the electron transport.

A simple method to determine the electrical properties of a metal | organic layer is to use a mercury drop[18-21] or an eutectic of Ga/In[22] to close the circuit (acting as the top-contact electrode). This technique is a simple, economic and fast system to verify the electrical properties of the film although it is not useful for making commercial devices. In addition, it is possible that the liquid metal can cause defects or reorganizations in the monolayer.[23,24]

Mechanically controllable break junction (MCBJ)[25] was first used in 1985 by Moreland and Ekin[26] to study the electron tunneling in atomic scale. Reed and Tour[27] used it again in 1997 to study the conductance of molecular junctions. Mechanically controllable break junctions use a notched metallic wire that is attached to a flexible substrate. Using a piezoelectric actuator, the substrate can be bent until the wire breaks at the notch and produces a gap. The separation of the junction's gap can be adjusted by the actuator, which allows the creation of a junction with adjustable width on a nanometer scale. After fracturing, molecules can be deposited (mostly, from a solution) on either or each of the electrodes. The electrodes are then brought together until one molecule bridges the gap between the electrodes. Using the break junction approach, the conductance properties of a wide variety of molecules can be studied. The main advantage of this technique is that you can make a high number of electrical measures. However, the disadvantages of MCBJ are also evident: the geometry and the configuration at the point where contact is made are often random and cannot be controlled by this technique. Theoretical calculations have shown that the geometry and configuration of the electrode surface influence the measure of the conductance of the single molecule.[28]

STM break junction[25,29] is a variant of MCBJ. Au STM tip, immersed in a solution of the molecules, is driven into and pulled back from an Au substrate. As the tip and substrate separate, a chain of Au atoms forms and, ultimately, breaks, allowing one or more molecules to be caught in the freshly formed gap. To obtain reproducible results with this method

conductance histogram approach is used. If a suitable sample has been prepared, the conductance histogram shows peaks at integer multiples of a fundamental conductance value, allowing, within the limitation of the spread of data, a fair estimate of the conductance (dI/dV) of a given type of single molecule. Using the STM break junction approach, the conductance of many different of single molecules, connected to two gold electrodes, can be studied. The conductance and tunneling current values obtain from the histograms are analyzed with computer programs. In conclusion, break junctions are formed by breaking a single metal wire into two sections leaving a gap between them. MCBJ and STM break junction, however, do not allow for any control over the exact shape of the electrodes and thus contact to the molecule under investigation. They do, however, provide some control on the width of the gap. So, with these techniques, gaps in the sub nanometer range can routinely be achieved, allowing single molecule measurements to be done, but not measurements in monolayers.

In 2001, Cui and Lindsay[25,30] report a reliable method (matrix isolation) for chemically bonding metal contacts to either end of an isolated molecule and measuring the *I-V* characteristics of the resulting circuit, matrix isolation. Molecules of 1,8-octanedithiol were inserted into an octanethiol monolayer [on Au(111)] using a replacement reaction whereby one of the two thiol groups becomes chemically bound to the gold substrate. The octanethiol monolayer acts as a molecular insulator, isolating the dithiol molecules from one another. The thiol groups at the top of the film were derivatized by incubating the monolayer with a suspension of gold nanoparticles. A gold STM tip was used to locate and contact individual particles bonded to the monolayer. *I-V* measurements made on over 4000 nanoparticles produced only five distinct families of curves. The curves correspond to multiples of a fundamental curve, lying on this fundamental curve when divided by the appropriate integer. The resistance of a single octanedithiol molecule was 900 ± 50 megohms, based on measurements on more than 1000 single molecules. In contrast, nonbonded contacts to octanethiol monolayers were at least four orders of magnitude more resistive, less reproducible, and had different voltage dependence,

demonstrating that the measurement of intrinsic molecular properties requires chemically bonded contacts.

The measurement of the electrical properties of molecules, down to the single molecule level, has recently become an experimental reality. So, in the past few years, at Liverpool University there has been developed and exploited novel scanning tunneling microscopy based methods for achieving this feat.[25,31,32] In these methods, a gold substrate is coated with a low coverage monolayer of molecules bearing two terminal thiol moieties; thiols interact strongly with gold. A gold STM tip is employed, and in the course of the experiments, one (or a few) molecule(s) forms a junction between tip and substrate, and the current through the junction is measured. In one implementation, which it is named the *I(s)* method, the tip is withdrawed from the substrate while the tunneling current is been measured. As they cannot know, a priori, how many molecules form the junction for any given experiment, many such measurements are made and the results are analyzed statistically to determine the current and the conductance through a single molecule. The main advantage of this method is that is the unique method that can be used to measure the conductance in monolayers. Later, they developed an alternative procedure, the *I(t)* method, in which a gold tip is held over the molecule covered Au substrate at a fixed distance while the tunnelling current is monitored. Jumps are seen in the tunnelling current, attributed to molecules forming and breaking contact. These jumps are similarly analysed statistically. This method is particularly advantageous for shorter molecules that are difficult to pick up using the *I(s)* method.

In conclusion, there are many different methods for measuring the electrical properties of metal | organic molecule | metal structures.

2- Fabrication of the top-contact electrode:

There are many different methods for making the top-contact electrode. In the following paragraphs, some of the most important techniques to fabricate the top-contact electrode in metal | organic layer | metal structures are described.

The simplest method is the evaporation of a metal onto the monolayer. However, this method generally produces the growth of metallic filaments (mushroom shaped structures) along the organic layer, short-circuiting the system.[33-36] A modification of this method which allows to reduce this problem is the evaporation of one metal on a cooled substrate (~100 K) introducing deflectors to block direct passage between the crucible, in which the metal is evaporated, and the sample; or introducing an inert gas into the evaporation chamber. The aim is to reduce the energy of the metal atoms which arrive at the surface of the monolayer.[37,38]

Other alternative is the deposition of a conductive polymeric layer onto the organic monolayer before evaporating the metal,[39] although in this case, the polymer can penetrate in the monolayer trough the holes or defects of the monolayer short-circuiting the system. Nano-transfer printing (nTP)[40] is other possible alternative. This method is based on the use of lithographic techniques for drawing patterns with atomic resolution in solid surfaces.[41-43] The main advantage of this technique is the reduction of short-circuits,[44] although it has limitations such as the necessity of making a real chemical bond between the terminal functional group of the molecule and the metal deposited limiting drastically the number of interfaces metal | molecule that can be used.[44] Other alternatives could be the use of a two-dimensional network of carbon nanotubes as the top-contact electrode (although the process is long, tedious and with inherent experimental difficulties),[45] the electrodeposition of metal (although frequently generate the growth of metallic filaments along the organic layer which short-circuit the system.[46,47] Finally, another alternative to make the top-contact electrode is by incubating monolayers, functionalized with a thiol terminal group, in suspensions of gold nanoparticles[48,49] although aggregation of the gold nanoparticles is not controllable and a complete metallization of the organic film is not achieved.

Therefore, we can conclude that new strategies to make the top-contact electrode without damaging the organic molecule or penetrating the film have to be developed to get stable and robust metal | organic molecule | metal devices.

Chapter 3: Instrumentation and materials

3.1. Instrumentation

3.1.1. Fabrication of Langmuir and Langmuir-Blodgett (LB) monolayers

Langmuir monolayers were fabricated in a Langmuir trough. The main components of a Langmuir trough are:[50] (i) a Teflon® cuvette, where the liquid subphase is placed, (ii) a mobile barrier, the element that allows the compression and the assembly organization of the molecules at the air-water interface, for making the bidimensional (2D) layer; (iii) a Wilhelmy balance,[51] to determine the surface pressure (π), which is defined as the difference between the surface tension of the clean subphase (γ_0), and the surface tension of the subphase covered by the monolayer (γ); and (iv) a dipper, where the substrates are placed for making the LB films. In this work, three different troughs were used. These troughs are situated in the Department of Physical Chemistry of the Faculty of Science: a homemade trough, with dimensions 210 x 460 mm^2;[52] a commercial trough from NIMA, with dimensions 100 x 720 mm^2; and a commercial KSV trough, that contains two troughs with dimensions 120 x 775 mm^2 each one and an effective total area of 240 x 775 mm^2. For preparing a Langmuir monolayer,[51,53,54] a known amount of the compound of interest is spread onto the liquid surface. After the complete evaporation of the solvent, the monolayer is compressed resulting in an array of molecules to form the 2D film. Once the Langmuir monolayer has an appropriate surface pressure for the transference, this monolayer can be deposited onto a solid substrate to obtain a LB film.[55] In a transfer process at a constant surface pressure, the transfer ratio[56] is defined as:

$$\tau = S_1 / S_0 \quad (1)$$

where S_0 is the geometric surface of the solid substrate and S_1 is the reduction of the area occupied by the film at the air-water interface during the transference process.

3.1.2. Characterization of the Langmuir-Blodgett (LB) films

In the following paragraphs, the equipment used in the characterization of the Langmuir-Blodgett (LB) films is described:

Atomic force microscopy (AFM): The equipment used to characterize the morphology and homogeneity of the LB films was an atomic force microscopy Multimode 8, from Veeco. This instrument belongs to the Advanced Microscopies Laboratory (LMA). The AFM creates images of the surface from the attraction and repulsion forces between the sample and the tip of the microscope. The system has a very thin tip which interacts with the sample surface, located at the end of a flexible sheet (cantilever). The tip sweeps across the surface and it is moved vertically by atomic forces, which are attractive or repulsive depending on the distance between the tip and the sample. Then, the software transforms this information into a two or three dimensional image. This technique provides information about the topography of the film at nanometric scale.[57] A silicon tip from Bruker with a constant force of 40 mN and operating at a resonance frequency of 300 kHz was used in this work. The images were recorded in high resolution (512 lines / sample) at a scan rate of 1 Hz, in air conditions and using the tapping mode.

Quartz crystal microbalance (QCM): The instrument used was a QCM200 balance from Stanford Research Systems that uses a QCM 25 sensor. The sensor is a thin α-quartz disk of 331 μm in thickness on whose surface circular are deposited gold electrodes on both sides. The nominal frequency of oscillation is approximately 5 MHz. The mode of operation involves applying an oscillating electric field between the crystal electrodes, which induces an oscillation that propagates through the quartz with a movement of the disc surface parallel to its side. The device is sensitive to disturbances produced in the surface, such as the deposition of a thin layer. The mass variation per unit area in the quartz crystal is related to the variation in the oscillation frequency of the crystal according to the Sauerbrey equation:[58]

$$\Delta f = - C_f \cdot \Delta m \qquad (2)$$

where Δf is the observed frequency change, C_f is the sensitivity factor of the crystal (in this work, C_f has a value of 56.6 $Hz \cdot \mu g^{-1} \cdot cm^2$), and Δm is the mass variation per unit

area. In particular, the quartz crystal microbalance was used to determine the transfer ratio and calculate the surface coating of the substrate on which the film was deposited.

UV-Vis spectroscopy (UV-Vis): The UV-Vis absorption spectra were obtained with a spectrophotometer Varian Cary 50 Bio UV-Vis. UV-Vis absorption spectroscopy is based on the absorption of radiation in the UV-Vis region by the molecule. This absorption of radiation is a consequence of the promotion of the electrons situated in the lowest energy orbitals. When the intensity of the incident beam (I_0) passes through the sample containing the chromophore, this intensity is attenuated up to the intensity of the transmitted beam (I). Thus, the fraction which has passed through the sample is called transmittance (T). The relationship between transmittance and absorbance is:

$$A = - \text{Log} (I / I_0) = - \text{Log} (T) \quad (3)$$

where A is the absorbance, I is the intensity of the incident beam, I_0 is the intensity of the transmitted beam and T is the transmittance. UV-Vis spectroscopy was used in this project to study the Langmuir-Blodgett (LB) films transferred onto quartz substrates. These substrates are situated perpendicular to the UV-Vis beam. The technique provides information about the molecular interactions in the films (presence or absence of aggregates, types of aggregates, etc.).[59] In addition, UV-Vis spectra of LB films can be used to determine if a monolayer, a bilayer, a trilayer,… was deposited.[60] Finally, the reduction of graphene oxide was studied by means of UV-Vis spectroscopy.

3.1.3. Electrical properties of the Langmuir-Blodgett (LB) films

The equipment used to determine the electrical properties of the fabricated metal | organic molecule | metal devices was:

Atomic force microscopy (AFM): The equipment used to determine the electrical properties was a conductive atomic force microscopy ICON, from Bruker. This instrument belongs to the Microelectronic National Centre of Barcelona (CNM) of the High Centre of Scientific Researches (CSIC) (Spain).[61] The equipment uses a Peak Force TUNA™ mode and a cantilever coated with Pt/Ir 20 nm, a spring constant of 0.4 $N \cdot m^{-1}$, a resonance frequency of 70 kHz and a tip edge size of approximately 25 nm, from Bruker. The measurements were carried out under humidity control, approximately 30 %, with N_2 flow. Before recording the *I-V* curves, a preliminary study

was carried out to check the influence of the applied set-point force in the deformation or damage of the monolayer.

3.2. Materials

In this project, four different materials have been used. On the one hand, see chapter 4, the materials assembled in Langmuir and Langmuir-Blodgett films have been the following: [[4-{(4-carboxy)ethynyl}phenyl]ethynyl]-(triphenylphosphine)-gold and the [1-isocyano-4-methoxy-benzene][4-amino-phenylethynyl]-gold, which we briefly call FOSGAC and G-PEA, respectively. The chemical structures of these compounds are shown in figure 1 and 2, respectively. These molecules have been synthesized at the Department of Chemistry of the University of Durham (United Kingdom) by the group of Professor Paul J. Low. The synthetic route and NMR spectra of these molecules can be found in references 62 and 63. These molecules have a hydrophilic terminal group (-COOH and $–NH_2$, respectively) that allows their anchoring at the water surface, and a hydrophobic portion which provides insolubility in water and stability to the Langmuir monolayers due to π-π interactions with side neighboring molecules.[62-65] From the point of view of the interest of these materials and their potential applications, there are two important points to be considered. Firstly, the strong conjugation of the –C≡C-Ph-C≡C-Ph-COOH and –C≡C-Ph-NH_2 groups that, as is well described in the literature,[73-75] is responsible of their remarkable electrical properties as molecular wires. However, the most significant aspect is the presence of the groups Ph_3P-Au-C≡ and CH_3-O-Ph-N≡C-Au-C≡, respectively. It has been observed that the presence of gold atoms could result in materials with memory properties.[62,63,66,67,68] In addition, the presence of a metal atom in the skeleton of this family of molecules can be used for fabricating GNPs which can be used as the top-contact electrode, without damaging the organic monolayer and penetrating the films, in metal | organic molecule | metal devices.[63,68,69] In this work, the electrical properties of devices incorporating these molecules have been determined.

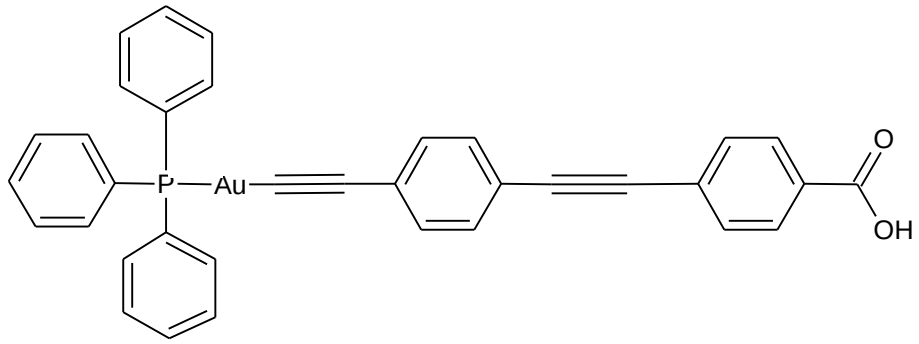

Figure 1. *Chemical structure of [[4-{(4-carboxy)ethynyl}phenyl]ethynyl]-(triphenylphosphine)-gold compound, FOSGAC.*

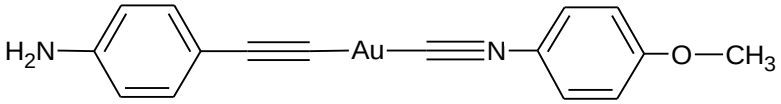

Figure 2. *Chemical structure of [1-isocyano-4-methoxy-benzene][4-amino-phenylethynyl]-gold compound, G-PEA.*

In chapter 5, graphene and 4-(4-(4-(trimethylsilylethynyl)phenylethynyl)phenylethynyl)-aniline, which we briefly call SOPEA, are studied. In figure 3 and 4 the chemical structures of these compounds are shown. SOPEA molecule was synthesized at the Department of Chemistry of the University of Durham (United Kingdom) by Professor Paul J. Low. The synthetic route and NMR spectra of this molecule can be found in reference 62. This molecule has a hydrophilic terminal group ($–NH_2$) that allows its anchoring on the water surface, and a hydrophobic portion which confers insolubility in water and provides stability to the Langmuir monolayers due to π-π interactions with side neighboring molecules.[62-65] Graphene was synthesized at the Instituto de Carboquímica de Zaragoza (CSIC)[70] by the group of Dra. Ana M. Benito and Dr. Wolfgang Maser. Graphene is a new interesting material with many different potential applications, including a large conductivity. Thus, graphene can be used as the top-contact electrode in molecular electronic devices avoiding the disadvantages[34] of the traditional methods used to fabricate the top-contact electrode. In this project, gold | SOPEA | graphene devices have been prepared.

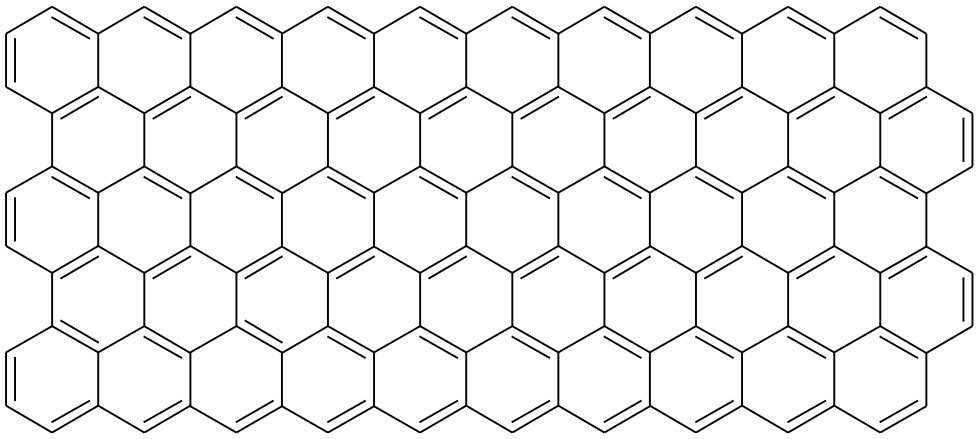

Figure 3. *Chemical structure of the graphene.*

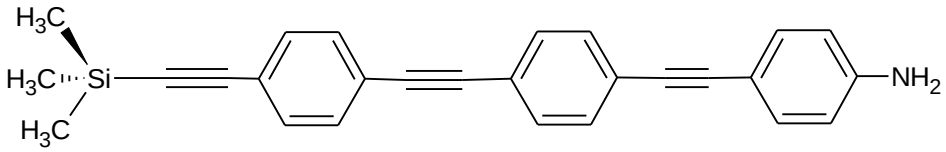

Figure 4. *Chemical structure of 4-(4-(4-(trimethylsilylethynyl)phenylethynyl)phenylethynyl)-aniline compound, SOPEA.*

Chemicals used in this work are shown in table I.

Tabla I. *Chemicals used in this project.*

Chemicals	*CAS*	*Commercial company*
Chlorofom	67-66-3	Sigma-Aldrich, 99 %. Stabilized with ethanol 1 %
Ethanol	64-17-5	Panreac, absolute, 99.5 %
Acetone	67-64-1	Panreac, QP, 99.5 %
Nitrogen	7727-37-9	Linde, 99.999 %

The different substrates used in this project together with the characterization technique and the cleaning sequence performed are shown in table II.

Tabla II. *Classification of the substrates in terms of the characterization technique used and the cleaning method.*

Substrate	*Commercial company*	*Characterization technique*	*Cleaning method*
Quartz	Hellma Analytics	UV-Vis spectroscopy (UV-Vis)	15 min in chlorofom with sonication. Drying with N_2. 4 times 15 min in pure water with sonication, rinsing with ethanol and drying con N_2
Mica	Ted Pella, Inc.	Atomic force microscopy (AFM) (topography)	Cleavage. Rinsing with ethanol. Drying
Gold	Arrandee®	Atomic force microscopy (AFM) (electrical properties)	Ethanol and drying with N_2
Quartz and gold	Stanford Research Systems	Quartz crystal microbalance (QCM)	Piranha solution[a]

[a] Piranha solution: mixture of hydrogen peroxide (H_2O_2) and sulfuric acid (H_2SO_4) in a 1:3 ratio. Peroxide is added over the acid. The mixture is very corrosive and reacts with organic matter, so the solution must be handled with appropriate protective measures.

Chapter 4: Electrical properties of FOSGAC and G-PEA

4.1. Langmuir and Langmuir-Blodgett (LB) monolayers and the fabrication of the top-contact electrode

The experimental conditions to prepare Langmuir and Langmuir-Blodgett monolayers as well as the fabrication of the top-contact electrode by using FOSGAC and G-PEA compounds have been the same as those used by myself in my final project degree (TAD)[68] and by Dr. Luz Marina Ballesteros Rueda in her PhD work,[63] respectively. Firstly, surface pressure-area per molecule isotherms of these molecules were fabricated to verify the reproducibility of the results previously obtained. In the case of FOSGAC, the preparation conditions of Langmuir films were: concentration of the spreading solution: $2.5 \cdot 10^{-5}$ M; solvent: chloroform; the solution was sonicated for 10 minutes; initial area per molecule: 1.60 $nm^2 \cdot molecule^{-1}$; compression speed: 0.018 $nm^2 \cdot molecule^{-1} \cdot min^{-1}$; and working temperature: 20 ± 1 ºC. The preparation conditions of G-PEA Langmuir films were: concentration of the spreading solution: $1 \cdot 10^{-5}$ M; solvent: chloroform; the solution was sonicated for 10 minutes; initial area per molecule: 2.30 $nm^2 \cdot molecule^{-1}$; compression speed: 0.018 $nm^2 \cdot molecule^{-1} \cdot min^{-1}$; and working temperature: 20 ± 1 ºC. In both cases a Millipore Milli-Q water (resistivity of 18.2 MΩ·cm) was used as subphase.

Once the monolayers of both compounds were formed at the air-water interface, these were transferred onto solid substrates for fabricating Langmuir-Blodgett (LB) films. FOSGAC monolayers can be transferred by withdrawing or dipping a substrate, having a Y-type transference and a transfer ratio close to one. The hydrophilic solid substrates were always withdrawn from the aqueous subphase to make the contact between the carboxylic acid of the molecule and the substrate. The upstroke speed was 7 $mm \cdot min^{-1}$ and the Langmuir films were transferred at a surface pressure of 10 $mN \cdot m^{-1}$. G-PEA monolayers can be only transferred during the withdrawn of the substrates, leading to Z-type LB films with a transfer ratio close to one. In this case, the hydrophilic solid substrates were also withdrawn from the aqueous subphase to make the contact between the amine group of the molecule and the substrate, the transfer

speed during the upstroke of the substrate was 7 $mm \cdot min^{-1}$ and the Langmuir films were transferred to a surface pressure of 16 $mN \cdot m^{-1}$. The obtained results for both molecules are in agreement with those obtained previously.[62,63,68]

It has been shown previously that these immobilized organometallic compounds decompose to generate, by annealing the LB film, gold nanoparticles (GNPs)which can act as the top-contact electrode in metal | organic layer | metal structures, figure 5.[63,68] Two different methods for generating these GNPs were tested (an irradiation process and a thermal process), getting the best results for the annealing process.[63,68] In the case of FOSGAC, the best conditions to generate GNPs are annealing at 150 ºC for 2 hours; meanwhile for the G-PEA the optimum conditions are annealing at 100 ºC for 2 hours. Figure 6 shows the XPS spectra of a pristine and annealed FOSGAC LB film. It is particularly interesting that this molecule contains a phosphorous atom which has a characteristic energy in the XPS spectrum that, as shown in figure 6, disappears after the annealing and subsequent rinsing processes, indicating that the triphenylphosphine group of FOSGAC is lost after the thermal treatment. In addition, the Au4f region for the film after the annealing process shows two peaks at 83.81 and 87.48 eV, attributable to Au(0)[71,72], whilst the pristine monolayer shows two intense peaks at 85.04 and 88.74 eV, attributable to Au(I),[73,74] and two weaker peaks at 83.88 and 87.56 eV attributable to gold (0) that is probably formed during the irradiation process required for the registration of the spectrum. On the other hand, figure 7 shows the XPS spectra of the Au4f region of G-PEA which confirms the reduction of Au(I) to Au(0) once the film has been annealed revealing that the annealing process is a general property of this family of compound and not just a specific feature of a compound.

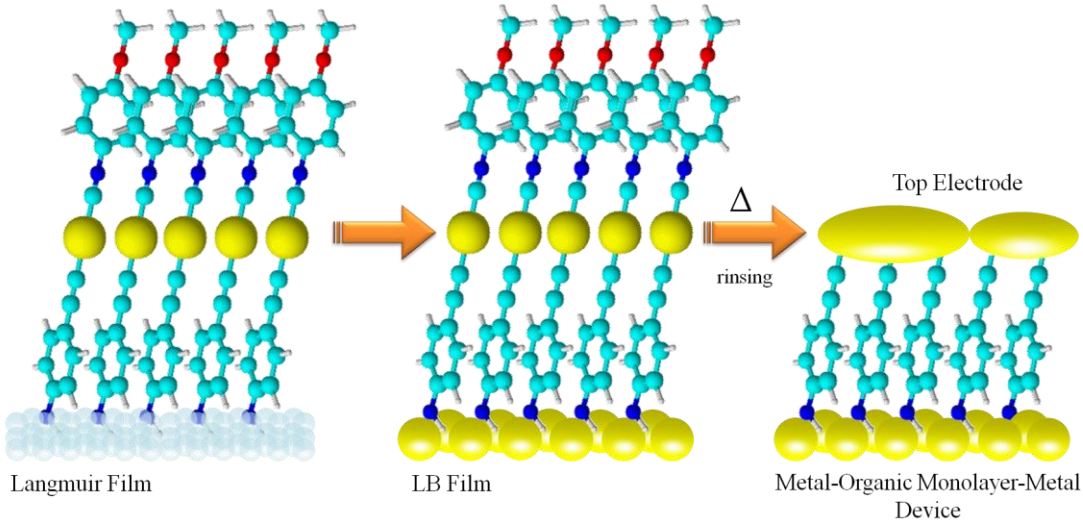

Figure 5. *Cartoon showing the method in which rupture of P-Au or C-Au bonds after annealing of immobilized monolayers occurs leading to the formation of gold NPs on the film surface (figure taken from reference 63).*

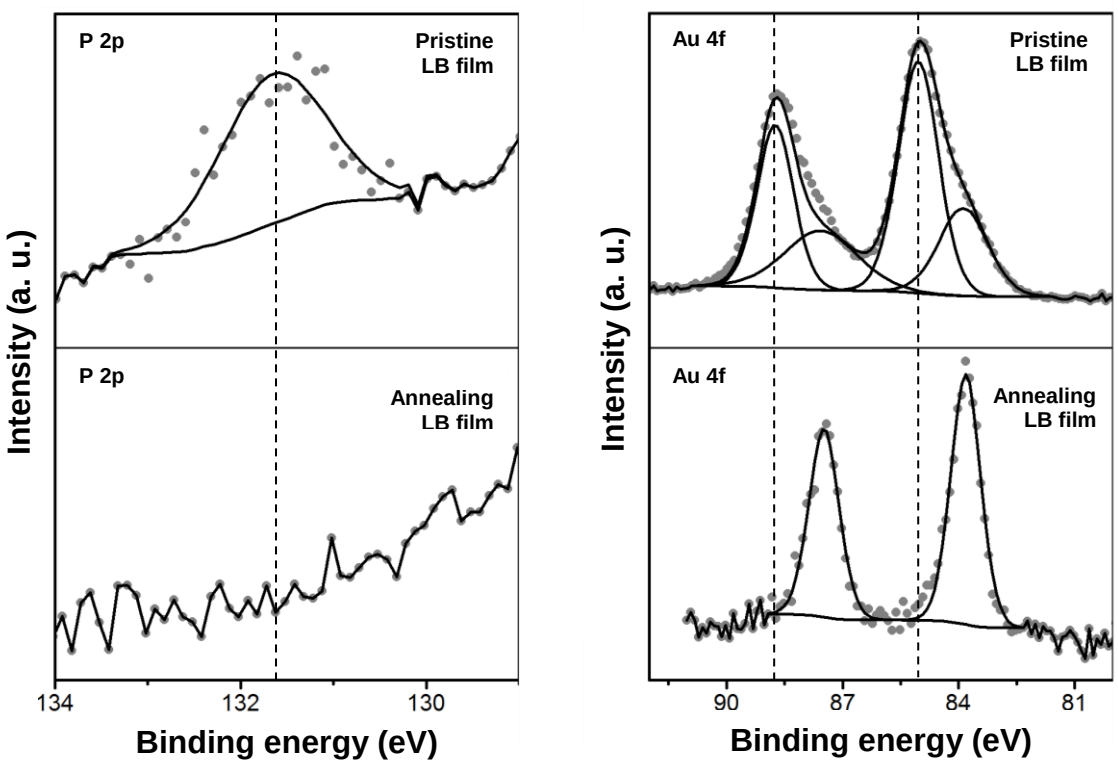

Figure 6. *XPS spectra in the region of P2p (left images) and Au4f (right images) for a FOSGAC monolayer transferred at 10 $mN \cdot m^{-1}$, before and after annealing the Langmuir-Blodgett (LB) film at 150 ºC for 2 hours (figure obtained of the reference 68).*

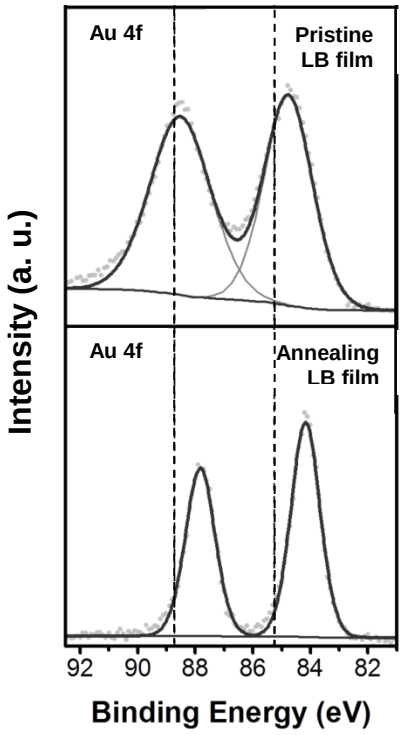

Figure 7. *XPS spectra in the region of Au4f for a G-PEA monolayer transferred at 16 mN·m^{-1}, before and after annealing the Langmuir-Blodgett (LB) film at 100 ºC for 2 hours (figure obtained of the reference 63).*

4.2. Electrical measurements

A frequent problem in the fabrication of the top-contact electrode is the formation of short-circuits due to a metallic contact between the bottom and top-contact electrodes.[34] Thus, it is really important to verify if the strategy proposed in the references 63 and 68 also leads to short-circuits or, on the contrary, is an effective strategy to avoid such problem obtaining metal | organic monolayer | gold nanoparticles (GNPs) systems without damaging the organic monolayer and penetrating the film. To probe the electrical properties of these metal | organic monolayer | gold nanoparticles (GNPs) sandwich structures fabricated as described above,[63,68] *I-V* curves were recorded with a conductive-AFM. The operation mode for the AFM (PF-TUNA™) was chosen, instead of a STM or conducting AFM in conventional contact mode, because it is a method for the conductivity mapping of soft or fragile samples since this technique avoids lateral forces during the images that would have damaged tip coating and sample surface, while at the same time allowing the use of cantilevers with low spring constant. Thus, the Peak Force Tunneling AFM used here combines "tapping" mode AFM with a conducting AFM tip and low-noise current amplifier to probe current flow through

these metal | organic monolayer | GNP junctions. Nevertheless, before recording the *I-V* curves, it is necessary to have a compromise in selecting the suitable peak force which is applied during the measurement: a rather small force would result in an inadequate electrical probing of the monolayer underlying the GNPs, while a too intense force would result in an unacceptably large deformation of the LB film. Therefore, before recording the *I-V* curves, control experiments were made to determine the most suitable set-point force monitoring the deformation or damage to the monolayer as a function of tip loading force (set-point force).

Figure 8 shows an AFM image of a FOSGAC LB film after the annealing process at 150 ºC for 2 hours using a set-point force of 1.5 nN. Three gold nanoparticles labelled as GNP1, GNP2, and GNP3 are clearly visible in the image.

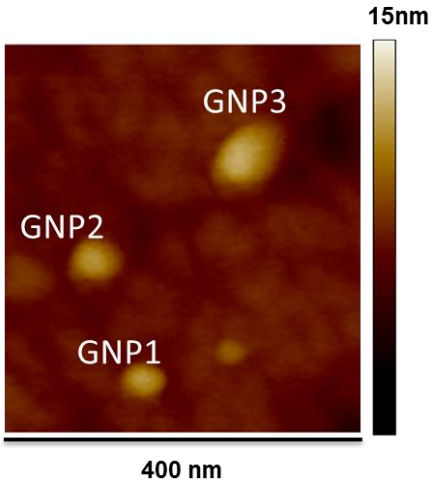

Figure 8. *AFM image of a FOSGAC LB film onto a gold substrate after annealing process at 150 ºC for 2 hours.*

When the applied set-point force is in the 1.5 to 17 nN range, the section analysis shows a practically constant height of 7.4, 9.0 and 8.9 nm for GNP1, GNP2 and GNP3, respectively (figure 9) revealing that in this set-point force range no deformation or damage of the monolayer occurs. However, if the set-point force is between 26 and 43 nN, a continuous deformation of the monolayer is observed since the section analysis shows heights of 6.8, 8.7 and 8.3 nm (at 26 nN) to 6.2, 8.0 and 7.7 nm (at 43 nN) for GNP1, GNP2 and GNP3, respectively. If the set-point force is turned to low values, for example to 8.75 nN, the section analysis of these GNPs shows heights of 5.1, 4.0 and 5.4 nm, which indicates that the deformation produced in the monolayer after applying a

high set-point force (43 nN) is reversible and does not induce damage in the organic layer.

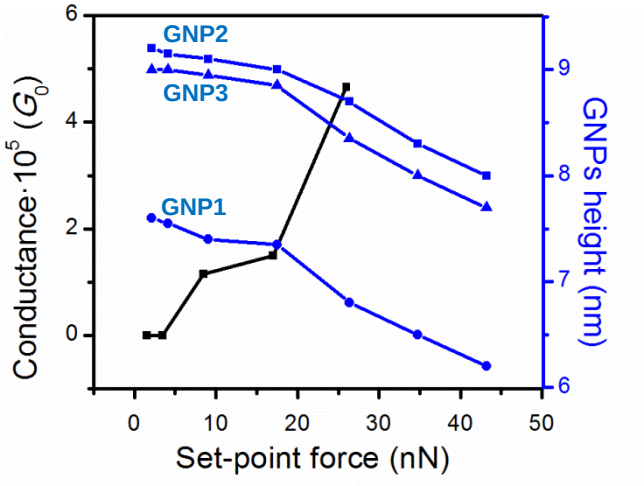

Figure 9. *Height of GNPs showed in figure 8 for an annealed FOSGAC film determined with the c-AFM at the indicated set-point forces together with the average conductance values measured by locating the tip of the c-AFM on the GNPs.*

After this study, the *I-V* curves were recorded for all range of the set-point forces used previously by sweeping the tip voltage (±1.2 V) once the c-AFM tip was located on the GNPs and a bias between the sample and the tip was applied with the LB-coated Au substrate held at ground. When the set-point force used is 1.5 or 3.5 nN no current was detected (figure 9). Meanwhile, if the set-point force is in the 3.5 to 17 nN range the *I-V* curves show low conductance suggesting that the contact between the tip and the GNP is not good. However, when a set-point force of 26 nN is used to record the *I-V* curves, the curves show a significant conductance (figures 9 and 10) revealing that for this set-point force the contact between the tip and the GNP is good. Therefore, this set-point force, 26 nN, was used to determine the electrical properties of these metal | organic monolayer | GNP junctions and to check the presence of short-circuits by recording the *I-V* curves. The *I-V* curves were averaged from multiple scans recorded for contacts to different GNPs, for ensuring reproducibility and reliability of the results, figure 10. These curves show a shape commonly observed for metal | organic molecule | metal junctions, with a linear section only at relatively low bias voltages (from -0.6 to +0.6 V, the ohmic region, where the conductance value is 4.65×10^{-5} G_0, where G_0 is the conductance quantum ($G_0=2e^2h \approx 77.4$ μS)) and increasing curve gradient at higher bias. In addition, and most importantly, only curves with this behavior were observed

and no low resistance traces characteristic of metallic short circuits were obtained over a wide range of set-point forces which rule out the presence of short-circuits.

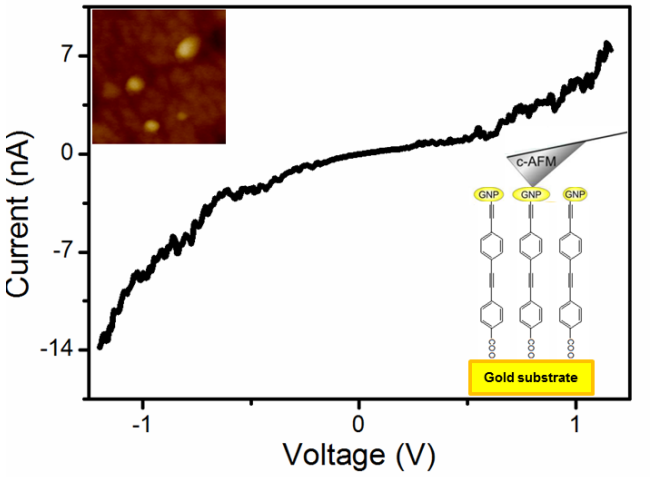

Figure 10. *Averaged I-V curve for the metal | FOSGAC monolayer | GNPs sandwich structures recorded using a set-point force of 26 nN. The inset top image shows a representative example of a 200 x 200 nm^2 image where gold NPs can be clearly distinguished and was used to position the c-AFM tip onto the NPs. The inset bottom image shows a scheme of the studied metal | organic monolayer | GNPs sandwich structures.*

Once the electrical properties of the metal | FOSGAC LB film | metal junctions were determined, a similar study is carried out for the G-PEA. Figure 11 shows an AFM image of a G-PEA LB film after annealing at 100 ºC for 2 hours using a set-point force of 3.5 nN. Three gold nanoparticles labeled as GNP1, GNP2 and GNP3 are clearly visible in the image.

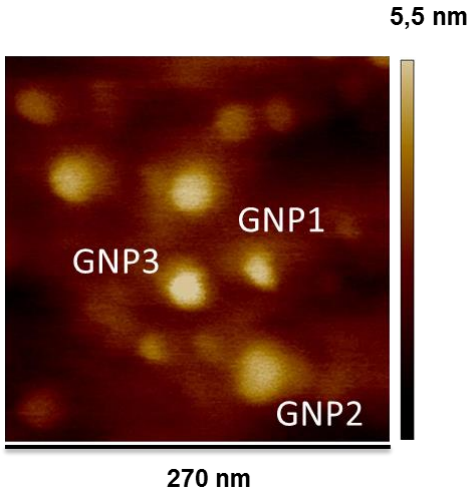

Figure 11. *AFM image of a G-PEA LB film onto a gold substrate after annealing at 100 ºC for 2 hours.*

When a set-point force in the range from 3.5 to 26 nN is applied, the section analysis shows practically constant heights of 5.2, 4.1 and 5.5 nm for GNP1, GNP2 and GNP3, respectively (figure 12). Thus, for this set-point force range no deformation or damage of the monolayer occurs. If the set-point force is increased up to 35 nN, the section analysis of the GNPs gives heights of 2.7, 2.4 and 4.4 nm for GNP1, GNP2 and GNP3, respectively, revealing that when this set-point force is applied there is a deformation of the monolayer. Finally, for a set-point force of 44 nN, the deformation of the monolayer increases since the section analysis shows heights of 2.1, 1.9 and 3.8 nm for GNP1, GNP2 and GNP3, respectively. Nevertheless, if the set-point force is turned to low values, for example to 8.5 nN, the section analysis of these GNPs shows heights of 5.2, 4.0 and 5.3 nm, which indicates that the deformation produced in the monolayer after applying a high set-point force (35 or 44 nN) is reversible and does not induce any damage in the organic layer.

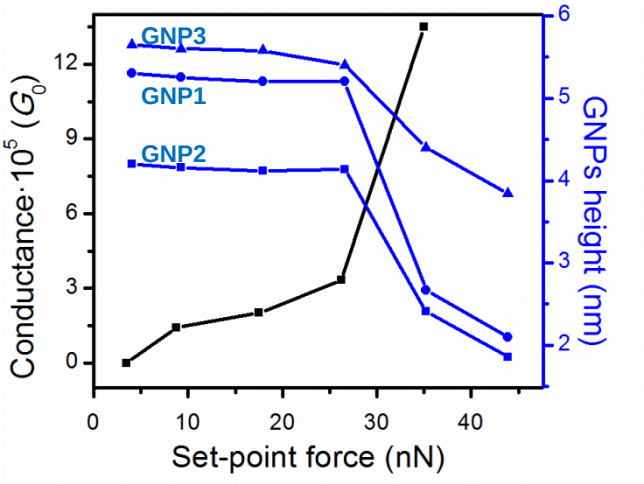

Figure 12. *Height of GNPs showed in figure 11 for an annealed G-PEA film determined with the c-AFM at the indicated set-point forces together with the average conductance values measured by locating the tip of the c-AFM on the GNPs.*

Once the influence of the applied set-point force in the monolayer was studied, the *I-V* curves were recorded for all range of the set-point forces used. When the used set-point force is 3.5 nN no current was detected (figure 12). Meanwhile, if the applied set-point force is in the range from 3.5 to 26 nN, the *I-V* curves show low conductance. These results suggest that when low set-point forces are used to record the *I-V* curves the contact between the tip and the GNP is not good. However, for a set-point force of 35 nN the *I-V* curves show a significant conductance (figures 12 and 13) revealing that

for this set-point force the contact between the tip and the GNP is good without damaging the monolayer. Therefore, the *I-V* curves were recorded for a set-point force of 35 nN. In figure 13 an averaged *I-V* curve for the metal | G-PEA monolayer | GNPs sandwich structures recorded as indicated previously for FOSGAC is showed. A similar behavior to this obtained for FOSGAC is observed which also rule out the presence of short-circuits in these structures. The conductance value is, in this case, 1.35×10^{-4} G_0 obtained from the linear section at relatively low bias voltages (from -0.6 to +0.6 V, the ohmic region).

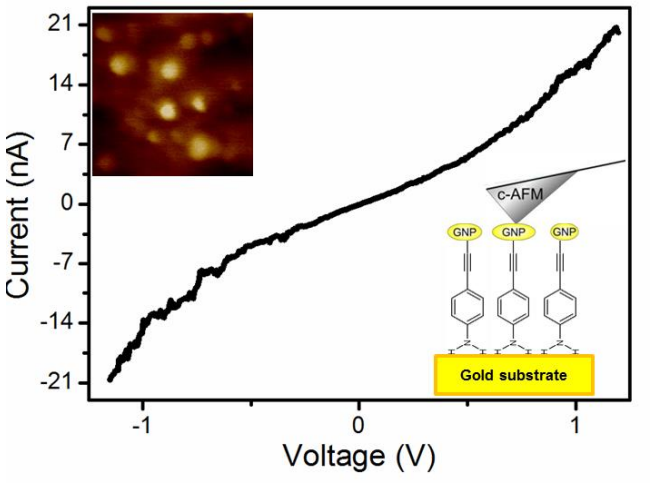

Figure 13. *Averaged I-V curve for the metal | G-PEA monolayer | GNPs sandwich structures recorded using a set-point force of 35 nN. The inset top image shows a representative example of a 200 x 200 nm^2 image where gold NPs can be clearly distinguished and was used to position the c-AFM tip onto the NPs. The inset bottom image shows a scheme of the studied metal | organic monolayer | GNPs sandwich structures.*

For these two metal | FOSGAC or G-PEA monolayer | GNPs sandwich structures, the electrical properties have been determined as an influence of the set-point force. *I-V* curves have not revealed evidences of short-circuits. Therefore, this new method for making the top-contact electrode, thermal induced decomposition of an organometallic compound, is an alternative system for solving the top-contact electrode problem without damaging the organic molecule, penetrating the film or altering/contaminating the interfaces.

Chapter 5: Graphene as top-contact electrode in molecular electronics

As mentioned previously, other important objective of this project is the development of a new strategy using graphene for making the top-contact electrode. In a previous work,[75] it was demonstrated that Langmuir and Langmuir-Blodgett films of graphene oxide solution can be fabricated. Therefore, we considered the possibility of using graphene oxide (GO) monolayers for making the top-contact electrode onto an organic monolayer after a chemical treatment of these layers to obtain reduced graphene oxide (RGO). Conjugated organic compounds have been widely used as molecular wires in molecular electronics.[7-9] In the last years, several organic compounds have been assembled using the LB technique to fabricate metal | LB film | metal (a STM tip) junctions in our group and their electrical properties were also determined.[76,77] Among all these compounds, SOPEA has been chosen to prepare a LB monolayer because this molecule has a hydrophilic terminal group ($-NH_2$) that allows its anchoring at the water surface, and a hydrophobic part which confers insolubility in water and provides stability to the Langmuir monolayers due to π-π interactions with side neighboring molecules.[62-65] This compound has been demonstrated to form very homogenous and stable monolayers at the air/water interface which can be transferred onto several substrates obtaining very homogenous films without holes or defect. In addition, these LB films are directionally oriented with good conductance values.[77] Therefore, the objective of this chapter is to fabricate a monolayer of SOPEA free of defects and to deposit a graphene oxide layer by the Langmuir-Blodgett (LB) technique as the top-contact electrode (figure 14) on top of the organic layer.

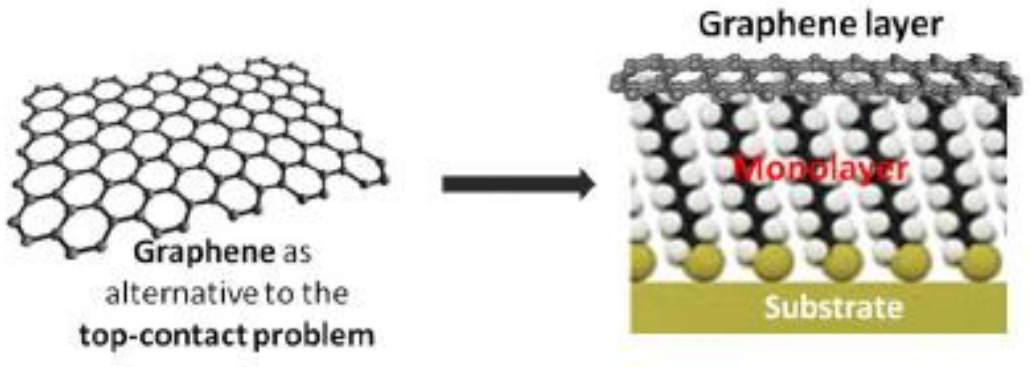

Figure 14. *Scheme of the metal | SOPEA monolayer | reduced graphene oxide sandwich structure.*

Nevertheless, to achieve this objective, different challenges had to be overcome. The first step was to reproduce the fabrication of the Langmuir and Langmuir-Blodgett (LB) films both of SOPEA and graphene under the same experimental conditions used previously in the group by Dr. Gorka Pera Seijo in his PhD[62] and Jorge Trasobares Sánchez in his final project master,[75] respectively. Once these films were fabricated under the same experimental conditions: spreading of a $1.0 \cdot 10^{-5}$ M solution in chloroform which was previously sonicated for 10 minutes, with an initial area per molecule of 2.50 $nm^2 \cdot molécula^{-1}$ and using a compression speed of 0.018 $nm^2 \cdot molécula^{-1} \cdot min^{-1}$ for SOPEA and spreading of a 8.8 $mg \cdot L^{-1}$ solution in water:methanol:chloroform (1:5:6), previously sonicated for 10 minutes with a compression speed of 7 $cm^2 \cdot min^{-1}$ for the graphene and using Millipore Milli-Q water as the subphase; the monolayers were transferred onto solid substrate to fabricate Langmuir-Blodgett (LB) films at 20 and 15 $mN \cdot m^{-1}$ for the SOPEA and graphene, respectively at a transfer speed of 7 $mm \cdot min^{-1}$. SOPEA films are Y-type, with a transfer ratio close to one. The transfer process was done during the upstroke of the substrate to favor the interaction between the amine group (NH_2) of the molecule and the substrate leaving the other end, the TMS group, free to interact with the graphene oxide layer in next steps.

Nevertheless, before carriying out the transference of graphene oxide onto a substrate containing the SOPEA LB film it was necessary to check firstly that a graphene oxide LB monolayer could be reduced successfully. A graphene oxide layer formed at the air-water interface was transferred onto a quartz substrate and the UV-Vis spectrum of the LB film was registered, figure 15. Afterwards, the graphene oxide LB

film was treated with hydrazine vapors[78] at the Instituto de Carboquímica de Aragón (CSIC) by Drs. Ana M. Benito and Wolfgang Maser. The UV-Vis spectrum of the reduced graphene oxide LB film was recorded, figure 15. The UV-Vis spectra of the graphene oxide (GO) layer shows a peak at 226 nm in agreement with the literature.[79] In addition, the LB film after the reduction treatment shows a peak at 263 nm associated to reduced graphene oxide (RGO).[79]

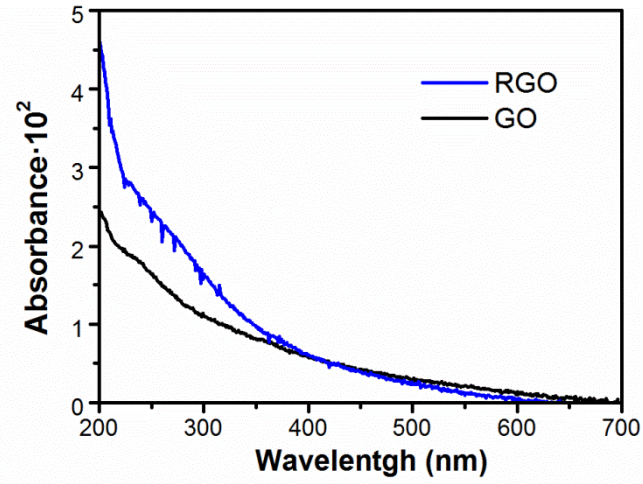

Figure 15. *UV-Vis spectra of a graphene oxide monolayer before and after the reduction treatment with hydrazine vapors.*

The open question now is if this treatment can damage the organic SOPEA LB film. To answer this question a monolayer of SOPEA was transferred onto a quartz substrate and the UV-Vis spectrum was recorded before and after the reduction with hydrazine vapors, figure 16. The pristine LB film shows a peak at 310 nm.[77] After the exposure to hydrazine, the UV-Vis spectrum of the LB film does not change, which demonstrate that hydrazine vapors do not damage the film.

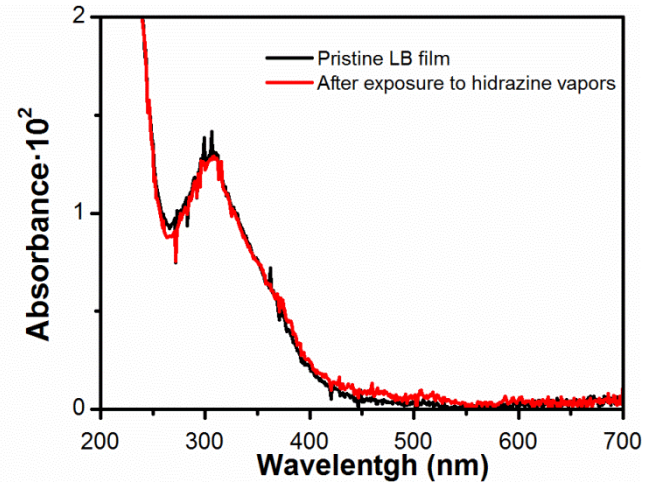

Figure 16. *UV-Vis spectra of a SOPEA monolayer pristine and after exposuring to hydrazine vapors.*

Once it has been demonstrated that the treatment with hydrazine vapors reduces the graphene oxide layer without damaging the organic monolayer, the next step was to transfer a graphene oxide layer onto a SOPEA LB film and its subsequent treatment with hydrazine vapours. A SOPEA monolayer was transferred onto a quartz substrate during the upstroke of the substrate. After that, a graphene oxide layer was transferred onto the organic SOPEA LB film and the UV-Vis spectrum of this structure was recorded, figure 17. The UV-Vis spectrum shows two peaks at 310 and 226 corresponding to the organic SOPEA monolayer[77] and the graphene oxide,[79] respectively, revealing the incorporation of the graphene oxide to the SOPEA LB film. Later, the SOPEA + GO layer was treated with hydrazine vapors to reduce the graphene oxide and the UV-Vis spectrum was registered to follow the process, figure 17. The peak at 310 nm corresponds to the SOPEA LB film, meanwhile the peak at 263 nm is due to the reduced graphene oxide (RGO). Therefore, UV-Vis spectroscopy has revealed the incorporation of graphene oxide onto the SOPEA LB film and its subsequent reduction to RGO without damaging the organic layer.

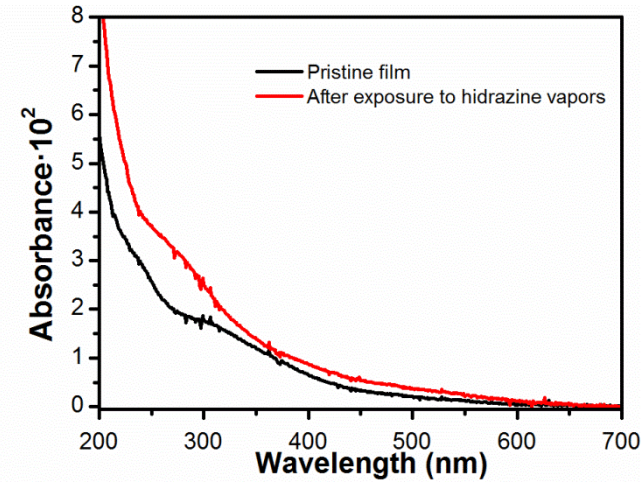

Figure 17. *UV-Vis spectra of Au-SOPEA-graphene oxide pristine and after the reduction process with hydrazine vapors.*

At this point it is necessary to indicate that the same study was carried out for LB films of SOPEA fabricated with the substrate initially outside of the aqueous subphase, hydrophobic substrate, to have the following structure: Au-TMS-OPE-NH_2, that is, leaving free the amine group to make the contact with the graphene oxide in order to check the influence of having different directionally oriented LB films. The same results were obtained indicating that both directionally oriented LB films can be used.

To confirm the results obtained with the UV-Vis spectroscopy, quartz crystal microbalance (QCM) experiments were carried out. Firstly, the frequency of a bare QCM substrate was determined, f_0, see table III. Afterwards, a monolayer of SOPEA was transferred onto these QCM substrates which were initially either inside or outside the aqueous subphase to have the two possible directionally oriented LB films: Au-NH_2-OPE-TMS, when the substrate is initially immersed or Au-TMS-OPE-NH_2 when the substrate is initially outside of the aqueous subphase; and the frequency was measured, f_1, in table III. The observed frequency change (f_0 - f_1) for both films, was 14 and 12 Hz for the Au-NH_2-OPE-TMS and Au-TMS-OPE-NH_2, respectively, which correspond to transfer ratios of 1.03 and 0.98 for the Au-NH_2-OPE-TMS and Au-TMS-OPE-NH_2, respectively, according to the Sauerbrey equation (2). Secondly, a graphene oxide layer was deposited onto the organic monolayer and the oscillation frequency was measured, f_2, in table III. The observed frequency change (f_1 – f_2) reveals the incorporation of the graphene oxide to the LB film as it has already been observed by

UV-Vis spectroscopy. Finally, these LB films were treated with hydrazine vapors to reduce the graphene oxide and the oscillation frequency was measured, f_3. The increase in the oscillation frequency with respect to f_2 suggests the elimination of the hydroxyl groups present in the graphene oxide as a consequence of the reduction of the graphene oxide layer in agreement with the spectroscopy results.

Table III. *Experimental results for the QCM experiments.*

Oscillation frequency of a QCM substrate	**Au-NH_2-OPE-TMS**	**Au-TMS-OPE-NH_2**
Bare susbstrate (f_0)	5007355 Hz	5007358 Hz
After deposition of a SOPEA monolayer (f_1) $\Delta f = (f_0 - f_1)$	5007341 Hz (τ = 1.03) Δf = + 14 Hz	5007346 Hz (τ = 0.98) Δf = + 12 Hz
After deposition of a graphene oxide layer (f_2) $\Delta f = (f_1 - f_2)$	5007270 Hz Δf = + 71 Hz	5007276 Hz Δf = + 70 Hz
After the treatment with hydrazine vapors (f_3) $\Delta f = (f_2 - f_3)$	5007286 Hz Δf = - 16 Hz	5007293 Hz Δf = - 17 Hz

Finally, the morphology of the different films transferred onto freshly cleaved mica substrates were evaluated by AFM imaging. Figure 18 shows an AFM image and section analysis profile of a one-layer LB film of SOPEA transferred onto a substrate initially immersed in the subphase, a mica-NH_2-OPE-TMS monolayer with the presence of aggregates of different size is observed; the film roughness, calculated in terms of the root mean squared (RMS), is 0.15 nm. Deposition of a graphene oxide film onto a mica-NH_2-OPE-TMS film, figure 19, shows a topography completely different to the one observed for the organic monolayer, figure 18, with an increase in the RMS (0.89 nm). Finally, an AFM image of the organic monolayer | reduced graphene oxide film is shown in figure 20. The image shows sheets of graphene with a constant height (3-4 nm), confirming the reduction of the graphene oxide as well as the presence of similar

aggregates to those observed in figure 19 indicating that not all graphene oxide is reduced by hydrazine vapors.

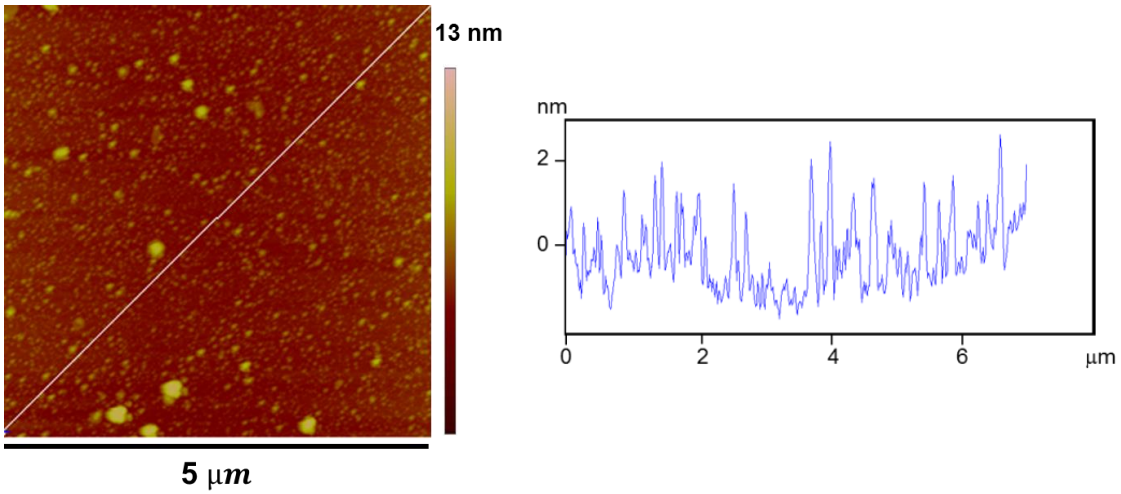

Figure 18. *AFM image and section analysis of mica-NH_2-OPE-TMS film transferred at 20 $mN \cdot m^{-1}$.*

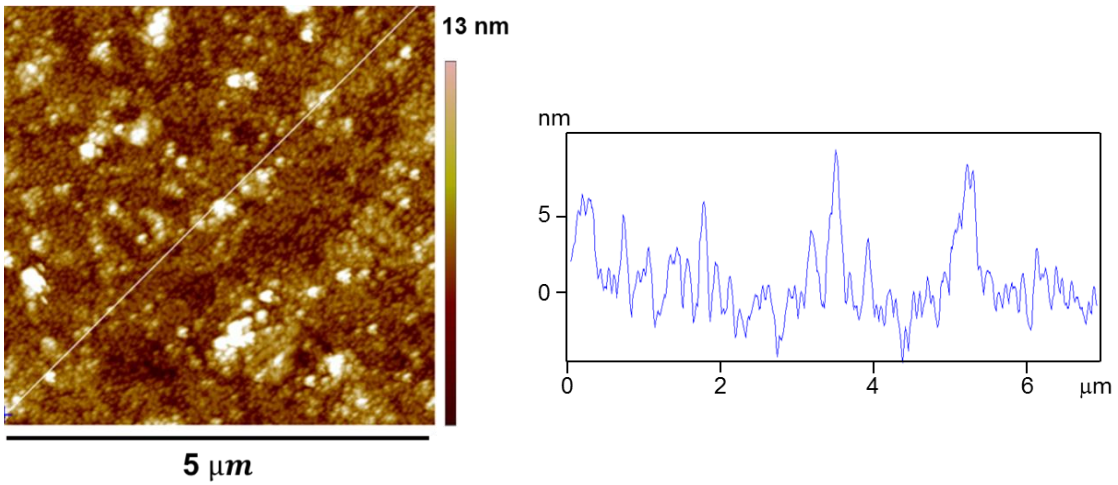

Figure 19. *AFM image and section analysis of mica-NH_2-OPE-TMS-graphene oxide film.*

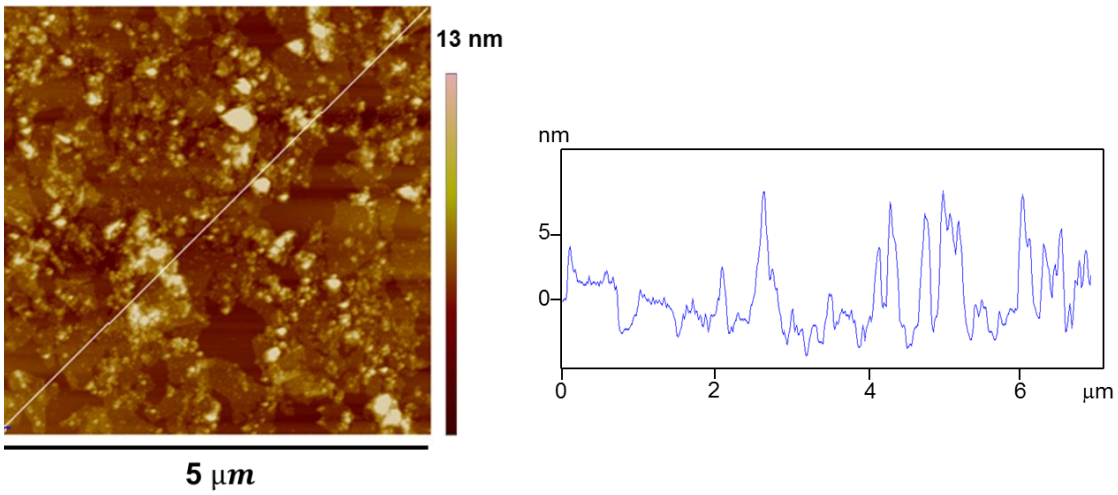

Figure 20. *AFM image and section analysis of mica-NH_2-OPE-TMS-reduced graphene oxide film.*

A similar study was carried out for a LB film of SOPEA transferred onto cleaved mica initially outside of the subphase (mica-TMS-OPE-NH_2) and the subsequent transference of a graphene oxide layer followed by treatment with hydrazine vapors, figures 21 to 23. As can be observed, similar results were obtained.

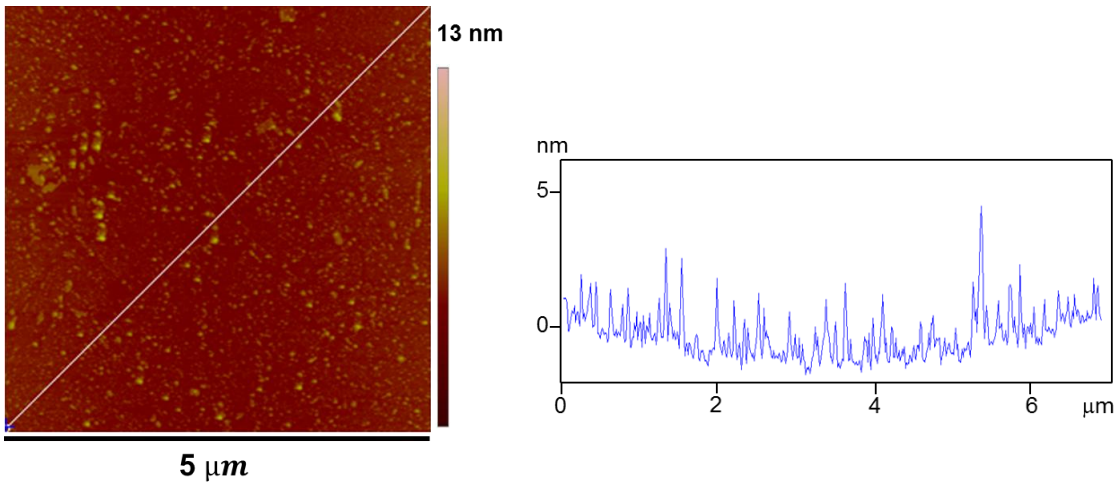

Figure 21. *AFM image and section analysis of mica-TMS-OPE-NH_2 film transferred at 20 $mN \cdot m^{-1}$.*

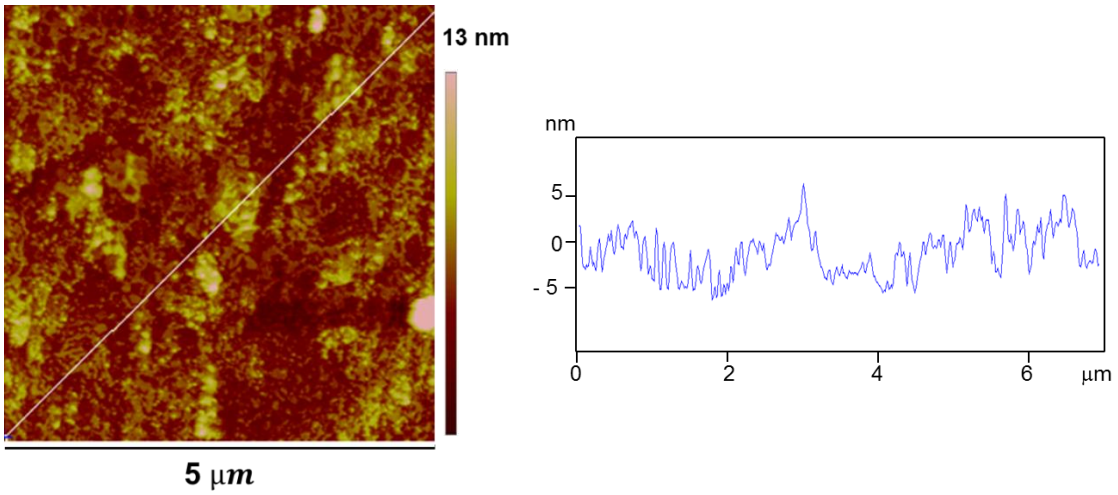

Figure 22. *AFM image and section analysis of mica-TMS-OPE-NH_2-graphene oxide film.*

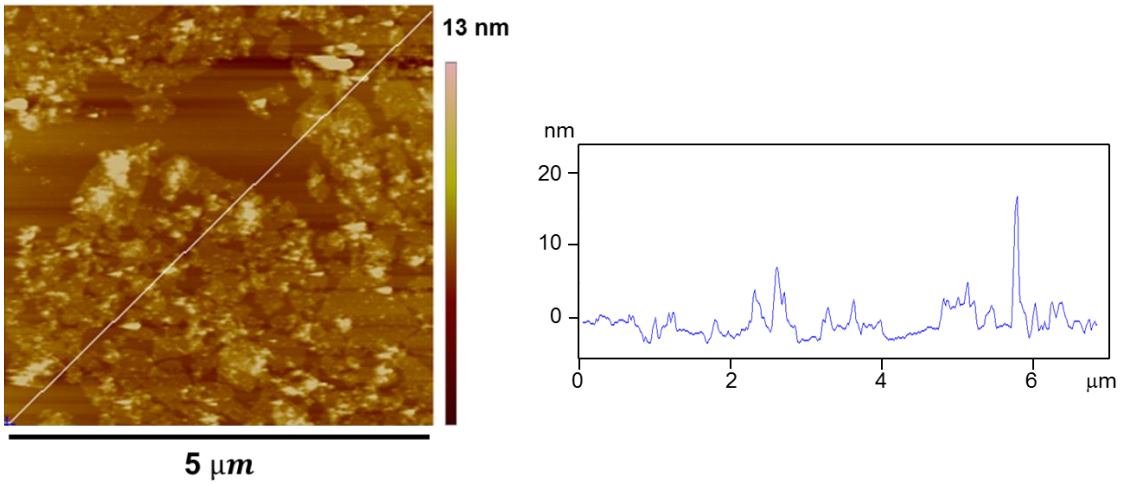

Figure 23. *AFM image and section analysis of mica-TMS-OPE-NH_2-reduced graphene oxide film.*

In conclusion, a new strategy using graphene has been considered to make the top-contact electrode in metal | organic layer structures without damaging the organic layer, being an alternative to other traditional methods. In this work a preliminary research of the possible use of graphene as the top-contact electrode in molecular electronics has been made, although further research is needed. In future projects, the following issues would be investigated: working with more homogenous organic films, to avoid the presence of aggregates, holes or defects in the monolayers; studying the organic layer | graphene junctions; trying to find new possible methods for reducing the graphene oxide; and measuring the electrical properties of the metal | organic film | graphene devices.

Chapter 6: Conclusions

In this section we will attempt to provide an overview of the experimental results obtained in this final project master:

Two organometallic compounds with a gold metal in their skeleton have been studied, FOSGAC and G-PEA. It was previously demonstrated that these immobilized organometallic compounds decompose to generate gold nanoparticles (GNPs) by annealing the LB films, and these GNPs could act as the top-contact electrode in molecular devices. In this work, the electrical properties of these metal | organic monolayer | GNPs sandwich structures have been determined as a function of the set-point force applied with a conductive-AFM to verify if the strategy proposed in references 63 and 68 also leads to short-circuits or on the contrary is an effective technique to avoid such problem, obtaining metal | organic monolayer | GNPs systems without damaging the organic monolayer and penetrating the film. *I*-*V* curves show a shape commonly observed for metal | organic molecule | metal junctions, with a linear section only at relatively low bias voltages and increasing curve gradient at higher bias. Only curves with this behavior were observed and no low resistance traces characteristic of metallic short circuits were obtained over a wide range of set-point forces which rule out the presence of short-circuits. Therefore, this new method for making the top-contact electrode, thermal induced decomposition of an organometallic compound, is an alternative system for solving the top-contact electrode problem without damaging the organic molecule, penetrating the film or altering/contaminating the interfaces.

A new strategy using graphene as alternative to other traditional methods has been developed to fabricate the top-contact electrode in metal | organic layers structures without damaging the monolayer. To achieve this objective, first, Langmuir and Langmuir-Blodgett monolayers of SOPEA and graphene oxide have been fabricated using the experimental conditions described in the literature. Then, a treatment with hydrazine vapors has been used to reduce the graphene oxide as it has been demonstrated by UV-Vis spectroscopy. In addition, UV-Vis experiments have demonstrated that this treatment does not damage the SOPEA film. Finally, metal | SOPEA LB film | reduced graphene oxide (RGO) structures have been fabricated as it has been demonstrated by UV-Vis spectroscopy, QCM and AFM.

Chapter 7: References

1. Ratner, M. *Nature Nanotechnology*, **2013**, *8*, 378.
2. Packan, P. *Science*, **1999**, *285*, 2079.
3. Aswal, D. K.; Lenfant, S.; Guerin, D.; Yakhmi, J. V.; Vuillaume, D. *Analytica Chimica Acta*, **2006**, *568*, 84.
4. Van der Molen, S. J. *Nature Nanotechnology*, **2013**, *8*, 315.
5. Frank, D. J.; Dennard, R. H.; Nowak, E.; Solomon, P. M.; Taur, Y.; Wong, H. S. P. *Proceedings of the IEEE*, **2001**, *89*, 259.
6. Likharev, K. K. *Nano and Giga Challenges in Microelectronics. Elsevier: Amsterdam*, **2003**.
7. Tao, N. J. *Nature Nanotechnology*, **2006**, *1*, 173.
8. Sedghi, G.; García-Suárez, V. M.; Esdaile, L. J.; Anderson, H. L.; Lamber, C. J.; Martín, S.; Bethell, D.; Higgins, S. J.; Elliot, M.; Bennet, N.; Macdonald, J. E.; Nichols, R. *Nature Nanotechnology*, **2011**, *6*, 517.
9. Villaume, D. *Comptes Rendus Physique*, **2008**, *9*, 78.
10. Lörtscher, E. *Nature Nanotechnology*, **2013**, *8*, 381.
11. Mann, B.; Kuhn, H. *Journal of Applied Physics*, **1971**, *42*, 4398.
12. Cuevas, J. C.; Scheer, E. *World Scientific*, **2010**, *1*, 3.
13. Heath, J. R.; Ratner, M. A. *Physics Today*, **2003**, *56*, 43.
14. Guédon, G.; Valkenier, H.; Markussen, T.; Thygesen, K. S.; Hummelen, J. C.; Van der Molen, S. J. *Nature Nanotechnology*, **2012**, *5*, 305.
15. Maruccio, G.; Cingolani, R.; Rinaldi, R. *Journal of Materials Chemistry*, **2004**, *14*, 542.

16. Marquardt, C. W.; Grunder, S.; Blaszczyk, A.; Dehm, s.; Hennrich, F.; Löhneysen, H. V.; Mayor, M.; Krupke, R. *Nature Nanotechnology*, **2010**, *5*, 863.

17. http://www.itrs.net/home.html

18. Rampi, M. A.; Schueller, O. J. A.; Whitesides, G. M. *Applied Physic Letters*, **1998**, *72*, 1781.

19. Holmlin, R. E.; Haag, R.; Chabinyc, M. L.; Ismagilov, R. F.; Cohen, A. E.; Terfort, A.; Rampi, M. A.; Whitesides, G. M. *Journal of the American Chemical Society*, **2001**, *123*, 5075.

20. Selzer, Y.; Salomon, A.; Cahen, D. *Journal of the American Chemical Society*, **2002**, *124*, 2886.

21. Selzer, Y.; Salomon, A.; Cahen, D. *Journal of Physical Chemistry B*, **2002**, *106*, 10432.

22. Chiechi, R. C.; Weiss, E. A.; Dickey, M. D.; Whitesides, G. M. *Angewandte Chemie International Edition*, **2008**, *47*, 142.

23. Slowinski, K.; Majda, M. *Electroanalytical Chemistry*, **2000**, *491*, 139.

24. Rampi, M. A.; Whitesides, G. M. *Chemical Physics*, **2002**, *281*, 373.

25. Nichols, R. J. *Master NANOMAT*, **2013**.

26. Moreland, J.; Ekin, J. *Journal of Applied Physics*, **1985**, *58*, 3888.

27. Reed, M. A.; Zhou, C.; Muller, C. J.; Burgin, T. P.; Tour, J. M. *Science*, **1997**, *278*, 252.

28. Basch, H.; Cohem, R.; Ratner, M. A. *Nano Letters*, **2005**, *5*, 1668.

29. Kumar, A. S.; Ye, T.; Takami, T.; Yu, B. C.; Flatt, A. K.; Tour, J. M.; Weiss, P, S. *Nano Letters*, **2008**, *8*, 1644.

30. Cui, X. D.; Primak, A.; Zarate, X.; Tomfohr, J.; Sankey, F.; Moore, A. L.; Moore, T. A.; Gust, D.; Harris, G.; Lindsay, S. M. *Science*, **2001**, *294*, 571.

31. Haiss, W.; Albrecht, T.; van Zalinge, H.; Higgins, S. J.; Bethell, D.; Hobenreich, H.; Schiffrin, D. J.; Nichols, R. J.; Kuznetsov, A. M.; Zhang, J.; Chi, Q.; Ulstrup, J. *Journal of Physical Chemistry B*, **2007**, *111*, 6703.

32. Nichols, R. J.; Haiss, W.; Higgins, S. J.; Leary, E.; Martin, S.; Bethell, D. *Physical Chemistry Chemical Physics*, **2010**, *12*, 2801.

33. Silien, C.; Buck, M. *Journal of Physical Chemistry C*, **2008**, *112*, 3881.

34. Villaume, D. *Proceedings of the IEEE*, **2010**, *1*.

35. Maitani Masato, M.; Allara David, L. *Topics in current chemistry*, **2012**, *312*, 239.

36. Walker, A. V.; Tighe, T. B.; Stapleton, J.; Haynie, B. C.; Upilli, S.; Allara, D. L.; Winograd, N. *Applied Physic Letters*, **2004**, *84*, 4008.

37. Xu, T.; Peterson, I. R.; Lakshmikantham, M. V.; Metzger, R. M. *Angewandte Chemie International Edition*, **2001**, *40*, 1749.

38. Metzger, R. M.; Xu, T.; Peterson, I. R. *Journal of Physical Chemistry B*, **2001**, *105*, 7280.

39. Akkerman, H. B.; Blom, P. W. M.; de Leeuw, D. M.; de Boer, B. *Nature* **2006**, *441*, 69.

40. Loo, Y.-L.; Lang, D. V.; Rogers, J. A.; Hsu, J. W. P. *Nano Letters*, **2003**, *3*, 913.

41. Hsu, C. C.; Chao, R. M.; Liu, C. W.; Liang, S. Y. *Journal of Micromechanics and Microengineering*, **2011**, *21*, 325.

42. Bareiss, M.; Ante, F.; Kalblein, D.; Jegert, G.; Jirauschek, C.; Scarpa, G.; Fabel, B.; Nelson, E. M.; Timp, G.; Zschieschang, U.; Klauk, H.; Porod, W.; Lugli, P. *ACS NANO*, **2012**, *6*, 2853.

43. Guerin, D.; Merckling, C.; Lenfant, S.; Wallart, X.; Vuillaume, D. *Journal of Physical Chemistry C*, **2007**, *111*, 7947.

44. Haick , H.; Cahen, D. *Progress in Surface Science*, **2008**, *83*, 217.

45. Li, T.; Hauptman, J. R.; Wei, Z. M.; Petersen, S.; Bovet, N.; Vosch, T.; Nygard, J.; Hu, W. P.; Liu, Y. Q.; Bjornholm, T.; Norgaard, K.; Laursen, B.W. *Advanced Materials*, **2012**, *24*, 1333.

46. Hagenstrom, H.; Schneeweiss, M. A.; Kolb, D. M. *Langmuir*, **1999**, *15*, 7802.

47. Xin, W. H.; Yang, L. L.; Zhao, J. P.; Li, Y. *Applied Surface Science*, **2012**, *258*, 7059.

48. Cui, X. D.; Primak, A.; Zarate, X.; Tomfohr, J.; Sankey, O. F.; Moore, A. L.; Moore, T. A.; Gust, D.; Harris, G.; Lindsay, S. M. *Science*, **2001**, *294*, 571.

49. Daniel, M.-C.; Astruc, D. *Chemical Reviews*, **2004**, *104*, 293.

50. Cea, P. Thesis (PhD), University of Zaragoza, *Estudio de moléculas orgánicas en películas de Langmuir-Blodgett*, **1998.**

51. Roberts, G. *Langmuir-Blodgett Films*. Plenum Press: New York, **1990**.

52. Royo, F. M.; López, M. C.; Ruiz, B.; Camacho, A.; Lozano, J. M.; Urieta, J., *Revista de la Academia de las Ciencias Exactas, Físicas, Químicas y Naturales de Zaragoza*, **1993**, *48*, 177-183.

53. Rideal, E. K. *An introduction to Surface Chemistry; Second Edition*. Cambridge University Press: Cambridge, **1930**.

54. Adam, N. K. *The Physics and Chemistry of Surfaces: Third Edition*. Oxford University Press: London, **1941**.

55. Blodgett, K. A. *Journal of American Chemical Society*, **1935**, *57*, 1007.

56. Langmuir, I.; Schaefer, V. J.; Sobotka, H. *Journal of the American Chemical Society*, **1937**, *59*, 71.

57. Haro, M.; Giner, B.; Lafuente, C.; Royo, F. M.; López, M. C.; Cea, P. *Langmuir*, **2005**, *21*, 2796.

58. Sauerbrey, G. *Zeitschrift fur Physik*, **1959**, *155*, 206.

59. Shukla, A. D.; Strawser, D.; Lucassen, A. C. B.; Freeman, D.; Cohen, H.; Jose, D. A.; Das, A.; Evmenenko, G.; Dutta, P.; Van, D. B. *The Journal of Physical Chemistry B*, **2004**, *108*, 17505.

60. Zhao, L.; Wong, K. M.; Li, B.; Li, W.; Zhu, N.; Wu, L.; Yam, V.W. *Chemistry – A European Journal*, **2010**, *16*, 6797.

61. http://www.cnm.es/

62. Pera, G. Thesis (PhD), University of Zaragoza, *Estudio de compuestos orgánicos altamente conjugados para la fabricación de nanodispositivos electrónicos*, **2011**.

63. Ballesteros, L. M. Thesis (PhD), University of Zaragoza, *Ensamblaje de moléculas orgánicas altamente conjugadas con potenciales aplicaciones en electrónica molecular*, **2012**.

64. Villares, A. Thesis (PhD), University of Zaragoza, *Fabricación de hilos moleculares mediante las técnicas de Langmuir-Blodgett y auto-ensamblaje*, **2008**.

65. Lin, P. H.; Guyot-Sionnest, P. *Langmuir*, **1999**, *15*, 6825.

66. Rath, A. K.; Dhara, K.; Banerjee, P.; Pal, A. J. *Langmuir*, **2008**, *24*, 5937.

67. Zhuang, X.-D.; Chen, Y.; Li, B.-X.; Ma, D.-G.; Zhang, B.; Li, Y. *Chemistry of Materials*, **2010**, *22*, 4455.

68. Cortés, J. Final Project Degree (TAD), University of Zaragoza, *Preparación de películas de Langmuir y de Langmuir-Blodgett (LB). Determinación de su estructura y aplicaciones*, **2012.**

69. Andrieux-Ledier, A.; Tremblay, B.; Courty, A. *Journal of Physical Chemistry C*, **2013**, *117*, 14850.

70. http://www.icb.csic.es/

71. Boyen, H. G.; Kästle, G.; Weigl, F.; Koslowski, B.; Dietrich, C.; Ziemann, P.; Spatz, J.; Riethmüller, S.; Hartmann, C.; Möller, M. *Science*, **2002**, *297*, 3.

72. Shan, C.; Yang, H.; Han, D.; Zhang, Q.; Ivaska, A.; Niu, L. *Biosensors and Bioelectronics*, **2010**, *25*, 4.

73. Bourg, M. C.; Badía, A.; Lennox, R. B. *Journal of Physical Chemistry B*, **2000**, *104*, 19.

74. Fratoddi, I.; Venditti, I.; Battocchio, C.; Polzonetti, G.; Cametti, C.; Russo, M. V. *Nanoscale Research Letters*, **2011**, *6*, 98.

75. Trasobares, J. Final Project Master (TFM), University of Zaragoza, *Use of highly conjugated organic compounds for the fabrication of metal / monolayer / metal devices*, **2012**.

76. Ballesteros, L. M.; Martín, S.; Pera. G.; Schauer, P. A.; Kay, N. J.; Lopez, M. C.; Low, P. J.; Nichols, R.; Cea, P. *Langmuir*, **2011**, *27*, 7.

77. Pera, G.; Martín, S.; Ballesteros, L. M.; Hope, A. J.; Low, P. J.; Nichols, R.; Cea, P. *Chemistry-A European Journal*, **2010**, *16*, 45.

78. Youn, S. C.; Geng, J.; Son, B. S.; Yang, S. B.; Kim, D. W.; Cho, H. M.; Jung, H. T. *Journal of Nanoscience and Nanotechnology*, **2011**, *7*, 64.

79. Castro-Beltran, A.; Sepulveda-Guzman, S.; De La Cruz-Hernandez, W. J.; Cruz-Silva, R. *Ingenierias*, **2011**, *14*, 52.